Building and Environment 293 (2026) 114376

Contents lists available at ScienceDirect

Building and Environment

journal homepage: www.elsevier.com/locate/buildenv

Cloud-based application for indoor daylight performance analysis through BIM-GIS Integration

Yangyu Liu, Eleonora Brembilla, Azarakhsh Rafiee *

Department of Architectural Engineering and Technology, Delft University of Technology, The Netherlands

ARTICLE INFO

Keywords:
Daylight simulation
BIM-GIS integration
Aperture-based daylight modeling (ABDM)
Cloud-based simulation
3D city model

ABSTRACT

Increasing urbanization intensifies daylight access challenges. Addressing this requires an integrated decision-making process that incorporates daylight considerations into urban design and planning. Integrated decision-making, from urban planning to building design and indoor performance, poses substantial challenges, such as data complexity, computational demand, conflicting objectives, and workflow integration. Integrating Building Information Model (BIM), Geographic Information Systems (GIS), and environmental simulation models creates an integrated decision-making platform with an intertwined design-feedback loop support. This study explores the design and development of a web application that combines script-based parametric modeling, cloud-based daylight simulation and geometry processing, and interactive geospatial visualization, allowing seamless BIM interaction to assess how dynamic changes in an urban environment affect daylight performance. This application computes façade-focused Aperture-Based Daylight Modeling (ABDM) metrics alongside traditional indoor-focused Climate-Based Daylight Modeling (CBDM) metrics. Our results demonstrate how to streamline daylight simulation to support building and urban design decision making.

1. Introduction

To address the increasing population and the resulting pressure on the housing market, many Dutch cities are planning significant expansions in housing. For instance, Amsterdam aims to build 7,500 new homes annually until 2035 [1]. The construction of new buildings can compromise the visual comfort of neighbouring occupants, particularly by reducing access to daylight and views. In the UK, this concern is formally addressed through the "Right to Light" law, which protects existing buildings from substantial loss of natural light due to nearby developments [2]. Visual comfort often involves a trade-off between various factors, and daylight simulation software is widely used to assess and compare different visual comfort parameters, with the goal of minimizing the negative impacts of new buildings during the planning phase [3]. In recent years, urban-scale daylighting research has gained increasing attention, with a strong focus on solar access, radiation analysis, and energy performance [4–6]. However, these studies often overlook the role of architectural elements and the reflective properties of building materials. This gap is significant, as material reflections can greatly influence daylight distribution and visual comfort in surrounding buildings—especially in dense urban settings where new developments alter existing light conditions.

Daylight simulation tools are essential for evaluating and optimizing natural lighting in architectural designs, playing a crucial role in enhancing occupant comfort, energy efficiency, and overall building performance. By providing accurate predictions of daylight distribution and intensity, tools based on Climate-Based Daylight Modeling (CBDM) allow designers to assess the impact on the interior environment of various design decisions, such as window placement, material selection, and building orientation [7]. Aperture-Based Daylight Modelling (ABDM) offers an alternative approach to assess the potential of a facade to admit daylight indoor, at early design phase, when the interior layout is yet to be decided on [8]. In the context of sustainability, effective daylighting can significantly reduce reliance on artificial lighting, contributing to energy savings and a lower environmental footprint [9,10]. Daylight simulation tools support the creation of healthier indoor environments by ensuring sufficient natural light, which has been linked to improved well-being, productivity, and mental health [11]. As urbanization increases and environmental concerns grow, the use of these tools becomes ever more important in achieving buildings that are both energy-efficient and conducive to occupant health.

A survey conducted by Fernandez-Antolin et al. in Spain [12,13],

* Corresponding author.
E-mail address: a.rafiee@tudelft.nl (A. Rafiee).

https://doi.org/10.1016/j.buildenv.2026.114376
Received 24 November 2025; Received in revised form 12 February 2026; Accepted 13 February 2026
Available online 14 February 2026

involving 157 architecture professionals, identified several barriers to the adoption of building performance simulation tools, such as complexity of use, excessive data input requirements [14], and inadequate user interfaces [12,13]. For these professionals, compatibility with computer-aided design (CAD) tools is the most important criterion. In real-world projects, architects must navigate a variety of daylight simulation tools, which can be overly complex [15]. Despite these challenges—and the fact that such tools are frequently requested by clients [12]—91.78% of young professionals with less than five years of experience reported having confidence in the simulation tools themselves [13]. This highlights the need for user-friendly simulation tools that offer clear guidance for optimal daylight analysis, especially amidst rapid urban development and increasing construction demands. Radiance, a validated physics-based ray-tracing engine, is behind most architectural software interfaces for daylight performance evaluation [16]. However, because different software platforms use varying methods, daylighting analysis requires the use of specialized, platform-specific simulation tools. This not only complicates collaboration within design teams but also impedes the sharing of results, hinders workflow integration, and increases the complexity of software learning.

1.1. Problem statement

In the field of urban planning, especially in the early stages of design and planning, the ability of users to interact with 3D city models through interfaces is critical for effective indoor daylighting simulations and for analysing the impact of additional buildings on existing buildings and vice versa. However, the current workflows and existing tools face several challenges. One major issue is the difficulty in user interaction with 3D city models. Additionally, integrating BIM with daylight simulation tools and GIS platforms is complex. This complexity hampers the intelligent identification and segregation of components by room, which is crucial for accurate and automated daylight simulation. As a result, users cannot interact efficiently with per-room BIM segments, reducing BIM's overall utility in daylight analysis. Furthermore, recently proposed ABDM metrics are promising indicators for urban-scale daylight studies but their correlation with more widespread CBDM metrics is yet to be tested. Lastly, the impact of detailed LODs on computational efficiency poses another challenge.

1.2. Research questions

The main research question is:

- To what extent can a web-based application perform per-room daylight analysis on BIM models to demonstrate the impact of dynamic urban context changes?
- To answer the main questions, the following research sub-questions have been investigated:
- How can 3D city models be served through the application interface, and how are these models loaded into Rhino for simulation and analysis?
- How can BIM models be integrated with Rhino and GIS to automatically identify room-level components and enable per-room daylight simulation and interaction?
- To what extent are ABDM metrics (SBI and view-lumen) suitable for urban-scale daylight analysis in terms of accuracy and simulation time compared to CBDM methods, and how can these be implemented and visualized in the application?
- How do different levels of detail (LODs) in 3D city models and spatial extent affect computational accuracy and performance, and how can the workflow be optimized for efficiency?

2. Related work

2.1. Indoor per-room daylight analysis

2.1.1. Urban canyon's impact

The geometry of adjacent buildings, such as their height, spacing, and orientation, as well as the reflective properties of their façade materials, are key factors influencing a building's access to daylight [17]. The use of highly reflective façade materials in newly developed buildings can help mitigate interior daylight losses in surrounding structures.

The Obstruction Angle (OA), typically defined as the angle between the horizontal ground plane and a line extending from the center of a window to the top of an adjacent building, is a well-established parameter in daylight assessment and planning guidelines [18]. OA serves as a practical tool for real estate developers to evaluate potential daylight performance and ensure compliance with regulatory standards during the early stages of urban design. In practical applications, when the existing building remains unchanged and only the surrounding context is altered, the OA is primarily affected by two factors: the roof type and the height of nearby buildings, including any proposed additions or roof modifications. Other important parameters influencing the amount of solar radiation and daylight reaching a building façade include the geometry of urban canyons, surface reflectance, external shading devices, street orientation, and the Sky View Factor (SVF) [19].

2.1.2. Daylight standard and metrics – CBDM & ABDM

Daylight metrics are quantitative measures used to evaluate the availability and quality of natural light in buildings, supporting design decisions that improve visual comfort, reduce energy use, and enhance occupants' well-being. Traditional standards relied on static measures such as the Daylight Factor, while modern Climate-Based Daylight Metrics (CBDMs) use annual climate data to capture variations in daylight throughout the year. CBDM evaluates daylight performance in buildings, typically measuring how often and how well spaces achieve useful daylight levels, accounting for location, orientation, and weather conditions [20]. This method has been used in different daylight performance applications [21–23].

European standard EN 17037 for daylight in buildings was approved in 2018 and became applicable to all participating countries in 2019 [24]. Although EN 17037 does not explicitly adopt defined CBDM metrics such as Daylight Autonomy (DA), spatial Daylight Autonomy (sDA), and Useful Daylight Illuminance (UDI), it introduces a daylight provision method based on similar climate-based simulation principles. DA measures the percentage of occupied time in which daylight provides the specified illuminance at a particular spot in a space, indicating daylight availability and non-reliance on electric lighting. sDA annually assesses the portion of a space that meets a certain DA target. The target, as set in this thesis paper, is 300 lux for at least 50% of the occupied time, as recommended by LEED v4 daylighting criteria [25]. The metric sDA is typically calculated using a daylight simulation that evaluates illuminance levels for every hour of the year, as defined by the IES LM-83-12 standard [26]. The UDI metric expresses the time frequency of annual illuminance falling into three ranges: insufficient (<lower bin), excessive (>upper bin), and autonomous (in between). Exceeding UDI values can cause issues like glare and overheating, while too little leads to insufficient illumination and reliance on electric lighting [27]. This research uses the typical thresholds of 100 lx and 3000 lux for the lower and upper bins respectively. In this study, sDA, DA, and UDI are selected as representative CBDM metrics due to their wide recognition in daylight performance evaluation and their conceptual alignment with the assessment method outlined in EN 17037, for further comparison between these established metrics and the proposed ABDM approach, within a European regulatory context.

ABDM introduces a novel approach to daylight simulation, focusing on assessing how effectively apertures connect with sunlight, with the sky and with the external environment [8]. ABDM offers the advantage of analyzing windows and potentially available daylight without requiring knowledge of the building's interior layout [8] highlighted the importance of this criterion in urban environments, noting its significant potential to make reasonable extrapolations of indoor daylight performance. This capability aids decision-making processes during the preliminary planning stages. This method also demonstrates potential for evaluating the impact of new housing developments on the daylighting of existing buildings. In theory, any 3D CAD/BIM tool capable of assessing on-site visibility between two points—one within the building model and the other representing the position of the sun on the sky dome—can compute Sunlight Beam Index (SBI) and Aperture Skylight Index (ASI) [28]. Consequently, the computations of SBI and ASI can significantly reduce computation time compared to traditional daylight analysis that accounts for inter-reflection via ray tracing. SBI provides a quantifiable estimate of potential sunlight availability, while the ASI is considered an indicator of skylight availability. These metrics are designed to measure the available daylight in urban settings, providing a clear quantification of how the outdoor environment impacts window daylighting capacity. Because this concept is relatively new, its application remains limited and only a small number of case studies and dedicated analytical tools exist to date. Recognizing this research gap, this paper aims to incorporate this new method into an urban planning design workflow. In the absence of defined target values within ABDM, results are discussed relative to annual daylight metrics like DA, sDA and UDI, bridging the gap between the ABDM method and conventional CBDM approaches.

[8] highlighted factors such as space types, obstruction scenarios, and climate conditions that need further investigation to provide calibration data for comparative assessments between CBDM and ABDM. In practice, room and window configurations involve variables that affect indoor daylight levels (e.g., windows number, orientation, and materials), consequently influencing the relationships among SBI, sky lumen, and daylight metrics such as DA, sDA, and UDI. In this study, simulations were conducted in room settings under varying conditions to investigate correlations between SBI, sky lumens (ABDM), and CBDM daylight metrics, while considering potential moderating variables (i.e., room size, layout, aperture height, shape, orientation, and the layout and number of apertures for a given total opening).

2.1.3. *Existing workflow for BIM daylight simulation*

Daylight simulation within BIM environments conventionally remains within the Revit ecosystem, using built-in or plugin-based solutions such as Autodesk Insight, AfterRad, IES Virtual Environment, and Honeybee integrated with Dynamo (Ladybug Tools[1]). These tools support varying degrees of daylight simulation and visualization, with Dynamo providing additional flexibility for parametric modeling and data extraction [29]. However, despite their accessibility, these workflows face key limitations regarding output formats and visualization capabilities. Results are typically exported as structured data files—such as XML, CSV, Excel, SDF, or SPD—without the ability to generate simulation visuals like images or 3D meshes. Visualization is generally confined to internal previews within the Revit interface, making it difficult to share results externally or integrate them into custom platforms or web applications. visualization tools. Additionally, both Revit and Forge are fundamentally tailored to building-level modeling and do not natively support large-scale Furthermore, the Forge Design Automation platform, which enables automated computational tasks within Revit, is primarily geared toward data processing and task automation rather than high-quality visualization. It does not support the generation or external hosting of detailed simulation outputs such as irradiance meshes, and users are restricted to viewing outputs via the Forge Viewer, which lacks compatibility with third-party urban geometries such as 3D city models. Formats like CityGML, OBJ, or GIS-based data are not well supported, which limits the scalability of these workflows in broader daylight simulation studies beyond individual buildings.

To overcome these limitations, this research adopts a workflow based on *Rhino.Inside.Revit*, which combines the BIM modeling capabilities of Revit with the flexible simulation and visualization environment of Rhino and Grasshopper [30]. This setup allows for the direct transfer of geometry and parameter data from Revit into Rhino, ensuring that essential BIM metadata is preserved throughout the simulation process. In contrast to translation methods like DXF or Speckle, which can result in the loss of semantic data or object relationships, this approach maintains data fidelity and improves workflow consistency. Within Rhino, advanced daylight simulations are performed using *Ladybug Tools*, and results can be visualized externally using *Rhino. Compute*. This cloud-based infrastructure allows for the hosting and interaction of simulation results via customized interfaces, making it easier to integrate daylight analysis into iterative design processes. A key advantage of this workflow is the potential for automation: rather than manually triggering simulations within Grasshopper, the setup enables simulations to be initiated through a user-facing web interface. This facilitates the efficient exploration of multiple design scenarios with minimal manual intervention. Finally, Rhino offers broader compatibility with large-scale urban geometries and GIS-based data, making it a more scalable and adaptable platform for daylight simulation tasks that extend beyond the building scale.

2.2. *3D city models and daylight analysis*

The availability and resolution of 3D city models are key considerations for urban environmental analysis, including daylight assessments. Currently, the most comprehensive standard for semantic 3D city models is CityGML (City Geography Markup Language), developed by the Open Geospatial Consortium[2] and the most used version is CityGML 2.0.

[31] recommend using LOD1.3 3D city models for daylight analysis, since most of the results show that both LOD2 and LOD1.3 yield similar OA-value results that don't differ more than 1° in most roof types. However, in neighborhoods characterized by buildings with gabled roofs, it should preferably be handled utilizing 3D city models whose LOD allows for a more detailed representation of the roof geometry as the difference in OA degrees sometimes exceeds 10°. LOD 1.2, 1.3, and 2.2 are supported by the regional database of Delft in the Netherlands [32]. In this research, LOD1.3 and LOD2.2 of the model will be used and compared.

2.3. *REST API-based daylight simulation*

Rhino, with its visual programming language GH are particularly popular choice for modern workflows working with parametric models. However, like many CAD tools, Rhino and GH have a high level of learning complexity, which limits their leverage in different applications and analyses. Sending the GH script to the designer's desktop and running it locally would require the designer to understand GH and properly set the correct inputs and outputs on the script canvas. This issue was also observed by Kohn Pedersen Fox (KPF), a leading architecture firm, in their implementation of digital workflows [33]. As 3D modelling and design grow more intricate, more designers and engineers are opting for cloud-based solutions to simplify their workflows and enhance collaboration with colleagues, clients, and other stakeholders (ShapeDiver[3]). Rhino Compute, unlike Rhino Desktop, can perform geometry calculations through a cloud based stateless REST API, and access 2400+ RhinoCommon API calls from outside Rhino, and provides

[1] https://www.ladybug.tools/

[2] https://www.ogc.org/standards/citygml/

[3] https://help.shapediver.com/doc/shapediver-rhino-compute

libraries with standalone C#(.NET), Python and JavaScript [30]. It is an open source project that enables running Rhino.Inside on a local server or in the Mcneel Rhino Compute cloud, allowing accessing Rhino and GH through a web API to run the program [34]. Rhino Compute reduces the entry barrier by simplifying complex workflows for typical architectural designers, while also offering greater flexibility for computational designers. As a geometry solver back-end, it enables the creation of user-friendly front-end applications that can be accessed via a web browser, allowing architects to execute complex parametric workflows with minimal technical effort [33].

2.4. BIM – GIS integration

The integration of Building Information Modeling (BIM) and Geographic Information Systems (GIS) has been recognized as essential for improving the efficiency, safety, and performance of complex urban infrastructure projects [35–38]. This integration is also becoming increasingly important for daylight simulation, as it enables a more holistic and accurate approach to assessing daylight access and performance in urban environments [39]. BIM provides detailed, geometrical and semantic data-rich models of individual buildings, while GIS offers a broader spatial context, including surrounding structures, topography, and geographic factors that influence sunlight exposure. Through their combination, designers and planners can simulate and analyze daylight conditions across both individual buildings and entire urban landscapes, accounting for factors such as solar radiation, shading, and site-specific climatic conditions. This integration enhances the precision of daylight simulations and enables better-informed design decisions. Moreover, BIM-GIS integration facilitates collaboration among multidisciplinary teams, allowing for a more seamless exchange of data and insights throughout the building lifecycle, from initial design to ongoing performance monitoring.

The reliability of daylight simulations depends on the geometric detail and accuracy of material properties used in the models. Insufficient levels of detail (LoDs) or inaccurate material data can compromise simulation outcomes and lead to misleading design decisions. Higher LoDs improve the realism of daylight simulations by better representing real-world features such as balconies, window frames, and façade articulations. However, they also increase model complexity and simulation time, especially at the urban scale. A balance between detail and efficiency is therefore essential for effective BIM–GIS integration in daylighting analysis [40].

However, a significant challenge to this integration is the inherently disparate data formats. When domain-specific data are not interoperable, they create data silos that restrict access to information and resources for other stakeholders. These data silos impede productivity, efficiency, innovation, and service quality [41]. Several available map libraries, including Mapbox[4], Cesium[5], and kepler.gl[6] require technical expertise to integrate map views into applications and to enhance their functionalities [42]. BIM integration with asset management and GIS technologies often results in isolated, non-interoperable systems, known as "island solutions". These integrations are typically platform-specific and lack scalability or extensibility [43,44].

2.5. BIM and simulation in Mapbox GL

Conventional BIM-GIS integration workflow mainly focus on the (static) visualization of BIM models on a GIS-based web platform, while not many applications can process and manipulate BIM models [45]. While some studies demonstrate BIM-GIS interactivity, models imported into GIS platforms typically behave as static visualizations, offering limited or no access to element-level properties or interactions. For instance, Revit models can be viewed in Mapbox using Autodesk Forge [46]. Additionally, BIM models can be positioned anywhere within Mapbox, with IFC properties accessible by clicking on elements before placement [47]. A tool for analyzing NYC parks[7] also integrates Rhino, Vue.js, Mapbox.gl, ApexCharts, Three.js[8], and Tailwind CSS[9]. The World Avatar project combines BIM and GIS within CesiumJS [42], and the CDC BIM campus digital twin is implemented using WebGL in a browser (CIMS Lab[10]).

The challenges of interacting with BIM data within MapboxGL are multifold. Objects in the model often lack proper alignment with the GIS coordinate system and do not retain their hierarchical or relational structure. As a result, the imported model is interpreted as a single undifferentiated geometry, rather than a collection of individuals, semantically rich components with distinct properties and relationships. When positioned using geodesic coordinates, individual objects face difficulties [45]. WebGL does not natively support any BIM format, necessitating conversion to a format that preserves semantic information alongside 3D geometries for further processing and supports interconnections between objects. Many BIM-to-GIS solutions are one-directional [43]. Additionally, converting between the Web-supported Mercator projection and geodesic coordinate systems presents another significant challenge [45].

2.6. Research scope

This research explores the system architecture design and development of an innovative cloud-based daylight simulation application, built within a WebGL-based 3D GIS platform to perform room-specific simulations using a BIM model. Users can interact with and modify the urban environment, such as adding new buildings, adjusting heights, and changing roof types. A major goal of this research is to explore how effectively the developed application can demonstrate the impact of dynamic changes in the urban environment, such as modifications in building typology, location, and surrounding structures, on daylight availability within individual rooms and how these insights can support informed urban planning and architectural design decisions. For this purpose, we explored the effective integration of BIM, a 3D GIS-based city model, and real-time daylight simulations within a unified WebGL-based platform. Through the developed web application, this research also quantitatively examines the relationship between ABDM metrics and CBDM annual metrics to ascertain whether SBI and ASI could serve as a proxy for indoor daylight performance, facilitating the simulation of indoor daylight in urban planning decision-making. This comparison is an integral part of the software development, as assessing the correlation between CBDM and ABDM metrics guides the incorporation of a proper metric into the developed application. This study implements ABDM capabilities in a building simulation interface for the first time. The impact of urban context extent on the performance of daylight simulations (through the developed application), in terms of accuracy and computational time, has been evaluated in this study.

3. Methodology and implementation

This research is centered around three primary themes: BIM, GIS, and daylight simulation (per-room), culminating in a web application that integrates these elements into a cohesive workflow. The workflow utilizes GH script as the back-end, Rhino Compute as the API connecting the front-end and back-end, and MapboxGL as the front-end and GIS platform for user interaction (Fig. 1). It includes the transformation

[4] https://www.mapbox.com/
[5] https://cesium.com/
[6] https://kepler.gl/
[7] https://nyc.emptybox.io/
[8] https://threejs.org/
[9] https://tailwindcss.com/
[10] https://cims.carleton.ca/project/Digital_Twin_Prototype

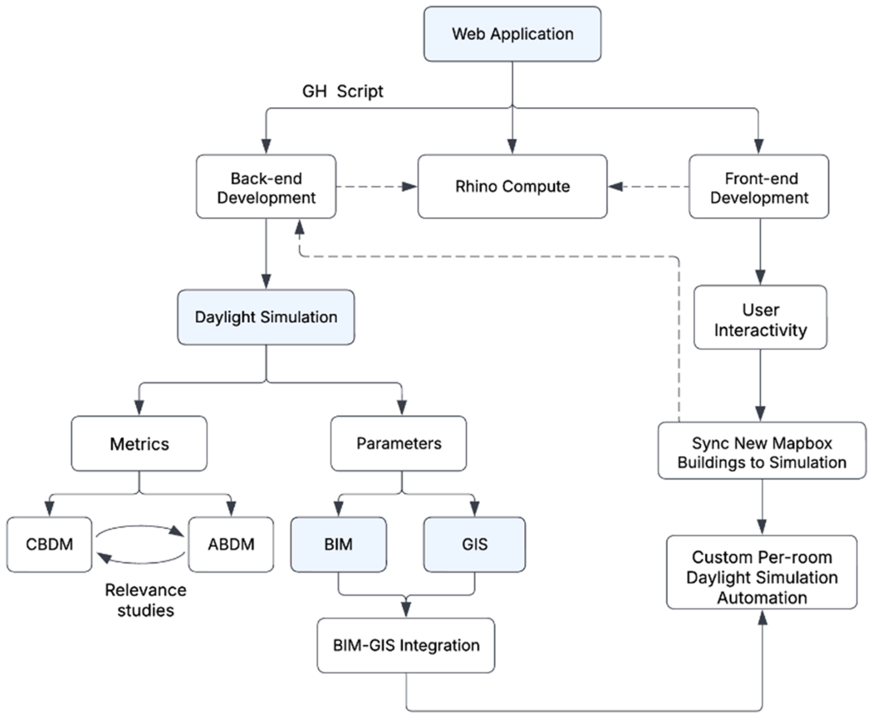

Fig. 1. Methodological framework.

process of semantic data and 3D geometrical information across multiple platforms. This study uses the BIM model of the Faculty of Architecture at Delft University of Technology as a case study.

The system is implemented as a web-based application that connects front-end user interaction, back-end processing, and cloud-based simulation through a Grasshopper script and Rhino Compute server. Building data and urban geometry are sourced from BIM and GIS datasets and integrated through a BIM-GIS interoperability layer, enabling consistent spatial referencing and geometry exchange. User-driven design changes, such as adding a building or modifying its geometry or material via an interactive map interface, are synchronized in real-time with the simulation environment. These updates trigger automated geometry processing and daylight simulations on the cloud, allowing scalable computation without local hardware constraints.

Daylight performance evaluation is conducted using two complementary metric families: traditional indoor-focused CBDM metrics and façade-focused ABDM metrics. CBDM metrics are computed per room using detailed BIM-derived interior models and standard climate-based simulations, serving as a benchmark for indoor daylight performance. In parallel, ABDM metrics are calculated at the façade level using exterior aperture characteristics and urban context, significantly reducing computational demand. The methodology enables studies that establish correlations between ABDM and CBDM metrics, testing ABDM's capabilities to function as a proxy for indoor daylight performance during early-stage urban design, where rapid feedback is critical.

The comparative approach in this study evaluates performance trade-offs between accuracy and efficiency by analyzing results from different LoDs and the spatial extent of surrounding buildings. Configuration parameters, including climate data, simulation settings, spatial resolution, and façade or room definitions, are managed within the back-end to ensure consistency across simulations. By integrating parametric modeling, cloud-based daylight simulation, and interactive geospatial visualization into a feedback loop, the proposed workflow addresses data complexity, computational scalability, and interdisciplinary integration, supporting daylight-aware decisions from urban planning to building design stages.

The developed platform enables users to interact with the web application, utilizing BIM data extraction workflow in MapboxGL and custom per-room daylight simulations, seamlessly integrating BIM into GIS for effective urban planning and design (Fig. 2).

3.1. Daylight simulations

This research combines the use of existing simulation tools with custom-developed scripts to evaluate daylight performance. For CBDM metrics, the simulations were conducted using off-the-shelf tools provided by the Honeybee plugin in Grasshopper. In contrast, for the simulation of ABDM metrics, custom Grasshopper scripts were developed specifically for this research, as these metrics are not yet implemented in existing tools. Following is the description of the applied daylight simulation metrics.

SBI has units of m^2 hours, and it works for any given period of time.

$$S_{\Delta t} = A_g coscos\,\theta\,\Delta t \tag{1}$$

In Eq. 1, the SBI value $S_{\Delta t}$ for a duration of time can be calculated by the direct sunbeam enters a glazed aperture of area A_g with an angle of incidence θ for a time period Δt [28]. The individual S_t values spanning the entire year can be utilized to populate a two-dimensional matrix, T (Eq. 2). For hourly data with a time step of 1 h, T possesses dimensions of 24 × 365.

$$T = \begin{bmatrix} S_{1,1} & \cdots & S_{1,365} \\ \vdots & \ddots & \vdots \\ S_{24,1} & \cdots & S_{24,365} \end{bmatrix} \tag{2}$$

ASI quantifies the degree of connectivity between an opening and the sky vault by assessing the illumination it receives from a uniformly bright sky dome, with the measurement averaged over the opening. As shown in Eq. 3, the illuminance of three layers of sky, ground and obstacle adds up to 2000lux [8].

$$2000 = E_{sky} + E_{obs} + E_{gnd} \tag{3}$$

And according to Eq. 4, the total lumens φ of an aperture with an area of A can be determined by multiplying A by the mean illuminance $\underline{E}$.

$$\varphi = \underline{E}A \tag{4}$$

The "lost" lumens refer to those lumens that are obscured due to the

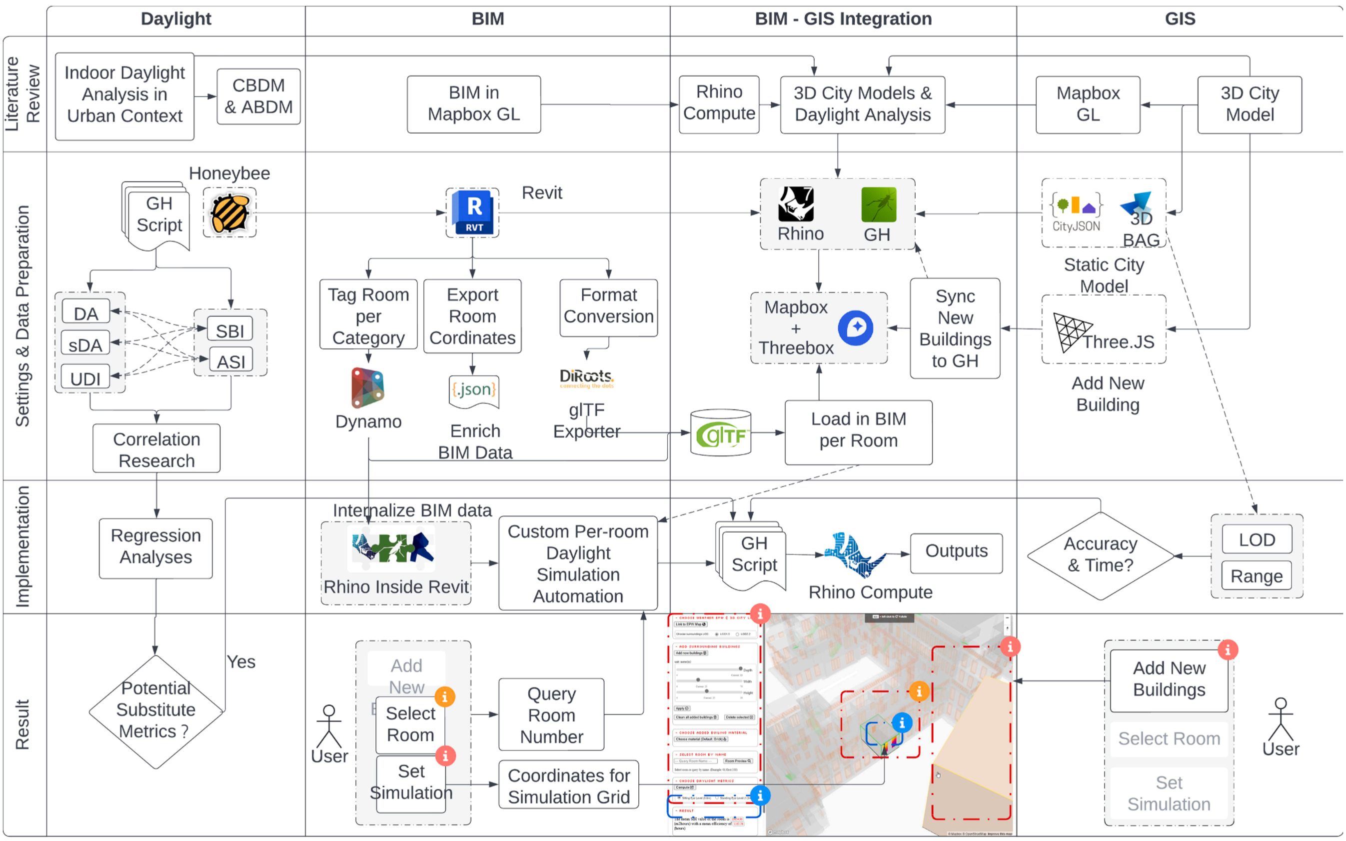

Fig. 2. System's components and their inter-relations.

shading effects of the reveal can be calculated using Eq. 5. φ_{sky}, which holds paramount importance in the study can be calculated in a similar approach.

$$\varphi_{lost} = 2000A - (\varphi_{sky} + \varphi_{obs} + \varphi_{gnd}) \tag{5}$$

In an apartment ABDM evaluation, the sky lumens lost through the balcony, overhang, and external obstruction can be calculated and visualized, and the actual lumen loss is always larger than that which seems apparent from the hemispherical image [8].

For ABDM metrics, to compute total annual SBI, the cumulative sum of SBI throughout the entire year with a sun altitude greater than 0 was computed. Following the recommendation of [28], a 15-minute time step is used to ensure sufficient solar position accuracy, with a maximum deviation of approximately 2.38°, which is comparable to that of a 9-minute interval, while maintaining computational efficiency. To address the substantial impact of low-angle sunlight on vertical apertures and its consequent effect on the SBI value, [24] proposed a revised formulation incorporating a new airmass coefficient, following the concept first introduced by [48]. This coefficient serves as an attenuation factor that characterizes the optical density of the atmosphere from sea level to the zenith. As a result, the original SBI-Classic formulation is updated to SBI-AM.

The calculation of this factor requires the solar constant, representing the solar irradiance outside Earth's atmosphere under air mass 0 conditions, which is 1.353 kW/m^2. The elevation level above sea level to calculate this factor is in km [49]. Another metric called SBI-efficiency can be calculated by dividing SBI by the area of the aperture.

In the case study of this research, all apertures of the BK building are perpendicular to the ground. Consequently, the angle of incidence (the angle between the sunlight and the window normal), is numerically equivalent to sun altitude. On the Netherlands topographic map, the elevation level of Delft, especially around the BK building, is 0.004 m. This also functions as the elevation input for LB Construct Location component in GH. Note that this input should be provided in meters.

To compute view lumen, the hemispherical fisheye view is of greater accuracy in depicting the illuminance received at the sensor point in comparison to the angular view [8]. Existing photo processing methods predominantly entailed the transformation of fisheye images into conventional viewpoints, thus, the techniques for generating hemispherical fisheye views and conducting subsequent color analysis emerged as the starting point for resolving this challenge. The approach adopted in this research employs the imaging principle of a hemispherical fisheye to construct circular geometric sensor units directly in Grasshopper. Inside these units, different segments corresponding to building projection, sky projection, ground projection, and shade projection are assigned specific colors. Subsequently, the area of each color-coded section was calculated, and its respective proportions within the sensor unit were assessed. This approach is inspired by Inanici's research [50]. The 3D geometry of the surrounding buildings is first projected onto a hemisphere that is perpendicular to the aperture plane. Subsequently, this projection onto the hemisphere is further transformed onto a circular sensor unit aligned parallel to the aperture. The combined illuminance contribution from the sky, ground, and obstacles adds up to 2000 lux, and the total lumens of an aperture can be determined by multiplying its area by the mean illuminance [8]. The "lost" lumens, which refer to those lumens that are obscured due to the shading effects of the reveal [8], are calculated by subtracting the combined contributions from the sky, obstacles, and ground from the theoretical total lumens. In the end, for any aperture of specific dimensions, the task is assessing the relative allocation of area occupied by different colored patches.

Our developed application supports the evaluation of daylight performance using annual daylight metrics, including DA, sDA, UDI, and the validated SBI metric. Users select the desired metric through a front-end interface, which triggers the retrieval of the corresponding simulation data and visualization settings. Depending on whether CBDM or ABDM is applied, the simulation grid is generated using either floor coordinates or window coordinates, respectively. For CBDM analyses, simulations are performed at predefined surface heights to represent typical workplane (0.80 m) and seated eye-level (1.20 m) conditions, enabling consistent and task-relevant assessment of indoor daylight availability.

The SBI method uses façade geometry, including apertures, to calculate a single SBI value for an interior space while processing multiple façade surfaces simultaneously. The result depends on aperture characteristics and how apertures are grouped within a defined space. Developed to reduce daylight analysis time, the method supports rapid evaluation in web-based tools and studies. Its main goal is to identify correlations between SBI or sky lumen values and standard CBDM metrics, enabling early estimation of CBDM performance using only exterior information—such as façades, apertures, shading, and surroundings—without detailed interior modeling or full simulations. Although SBI cannot replace CBDM, required for certifications like LEED, it provides a fast, computationally efficient means to support early design decisions and reduce simulation effort.

3.2. BIM-GIS-daylight simulation integration

The initial phase of the workflow involves the preparation and integration of data from Building Information Modeling (BIM) and Mapbox. This process can be divided into three main steps: (1) extracting room-related information from BIM elements and preparing it for import into Rhino, (2) importing the interactive BIM model into the Mapbox platform, and (3) synchronizing user-generated buildings in Mapbox with the backend Grasshopper system. The integration of BIM data into WebGL follows the workflow established by [51]. This process begins by separating BIM data into geometric and non-geometric (semantic) components. The geometric data is then converted into the open standard glTF format, which is an efficient, interoperable format for transmitting 3D models and scenes, well-suited for web applications and real-time rendering environments. Non-geometric (semantic) data, is exported as lightweight JSON files, which are linked to the corresponding geometric elements via unique "Element IDs." This separation and subsequent linking of data improve the flexibility and efficiency of the data integration process. The geometric relationships are established using bounding boxes, such as determining whether a bounding box contains a center point or intersects with another bounding box. The methodology also incorporates filtering elements and automating processes for each room, including the conversion of the BIM model into Grasshopper. A challenging aspect of this approach is managing inputs and outputs within Rhino Compute to ensure that simulation results are displayed at the correct coordinates on the front end.

Upon the selection of a room by the user, in the front-end interface, the room number is extracted and sent to Rhino Compute as input. The room number and its category name are then queried within GH on the back-end to distinguish between the different rooms for sunlight simulation. To simulate sunlight accurately, the geometry of each room is processed to differentiate between its components and apply the appropriate materials. Notably, since ceilings are not predefined as a separate category in BIM, they are created by duplicating and offsetting the floor geometry.

The integration of per-room daylight simulations consists of several stages, including the front-end, back-end, data processing, and Rhino Compute (Fig. 3). Upon user input, the data is transmitted to Rhino Compute in the form of integers, numbers, and strings. Based on the selected Level of Detail (LOD) and desired metrics, Rhino Compute identifies and executes the appropriate GH script. Subsequently, the server performs sunlight simulation according to the instructions specified in the GH script. Additionally, when the user adds extra buildings in Mapbox, data such as coordinates, materials, rotation angles, and other attributes are transmitted as lists. This ensures that null values are avoided, even in cases where certain building types are missing.

To assess the impact of alternative design scenarios and support informed urban planning and design decisions, comparative analysis of daylight simulations enables systematic evaluation of how different building configurations and simulation parameters affect daylight availability. In this application, for each simulation run, the resulting daylight performance data are temporarily stored, enabling direct comparison with subsequent simulations. This approach allows users to evaluate and contrast multiple design scenarios under consistent environmental conditions. As a result, the platform supports iterative design exploration and informed decision-making regarding daylight performance.

3.3. Workflow optimization

To optimize the workflow, it is essential to compare the impacts of different Levels of Detail (LODs) as well as the coverage range of 3D city model on the simulation performance. This benchmark comparison assesses both the time efficiency and accuracy of daylight simulations using LOD 1.3 and LOD 2.2. It is assumed that LOD 2.2 yields more accurate results due to its inclusion of more detailed roof information, which enhances the precision of the Open Area (OA) values used in per-room daylight simulations (Eq. 6).

$$\text{Percentage Difference} = \frac{|ValueLOD\,1.3 - ValueLOD\,2.2|}{Value_{\text{LOD2.2}}} \text{x}100\% \tag{6}$$

To optimize the workflow, the influence of the spatial extent of surrounding buildings on the accuracy and computational duration of daylight simulations is also evaluated. The geometric center of the BIM model was used as the origin for range radius expansions, encompassing 200m, 250m, 300m, and 350m (Fig. 4).

The benchmark for simulation accuracy regarding radius is based on the 350m range radius. This range is considered the most accurate as it encompasses the most extensive model information, ensuring a comprehensive analysis of the surrounding buildings' impact on daylight simulation. Therefore, all other radius options (200m, 250m, and 300m) are evaluated against the 350m radius to determine their effectiveness and efficiency. The ground average reflectance was set as a standard value of 0.20.

4. Results and discussions

4.1. User Interface design and workflow for daylight simulation

Fig. 5 illustrates the User Interface design of our developed platform.

The first step involves setting up the static urban environment and selecting the site-specific EnergyPlus Weather (EPW) data, which typically do not require frequent adjustments. The current implementation allows users to manually obtain EPW file links by selecting a location and copying the associated link. The second step features a drop-down menu offering three prototypes for adding new buildings. These buildings are initially positioned in a default location and can be resized using a slider. Users can preview adjustments. All newly added buildings or selected ones can be deleted by the user. In the third step, users can modify the materials of the newly added buildings, choosing from three available options. Material changes can be previewed in Mapbox, with corresponding color changes. Users can click on any newly added building to view its material information. The fourth step involves selecting the room for simulation. Rooms can be queried either by name (through the drop-down menu) or upon clicking. In the latter case, the bounding box in Threebox is automatically generated upon a hover or click event. Upon selecting a room by the user, or conducting a query and opting to "preview Room," the unselected segments of the BIM model are rendered 97% transparent to emphasize the selected room visually. The fifth step requires selecting metrics from a drop-down menu for sunlight simulation and setting the simulating surface height

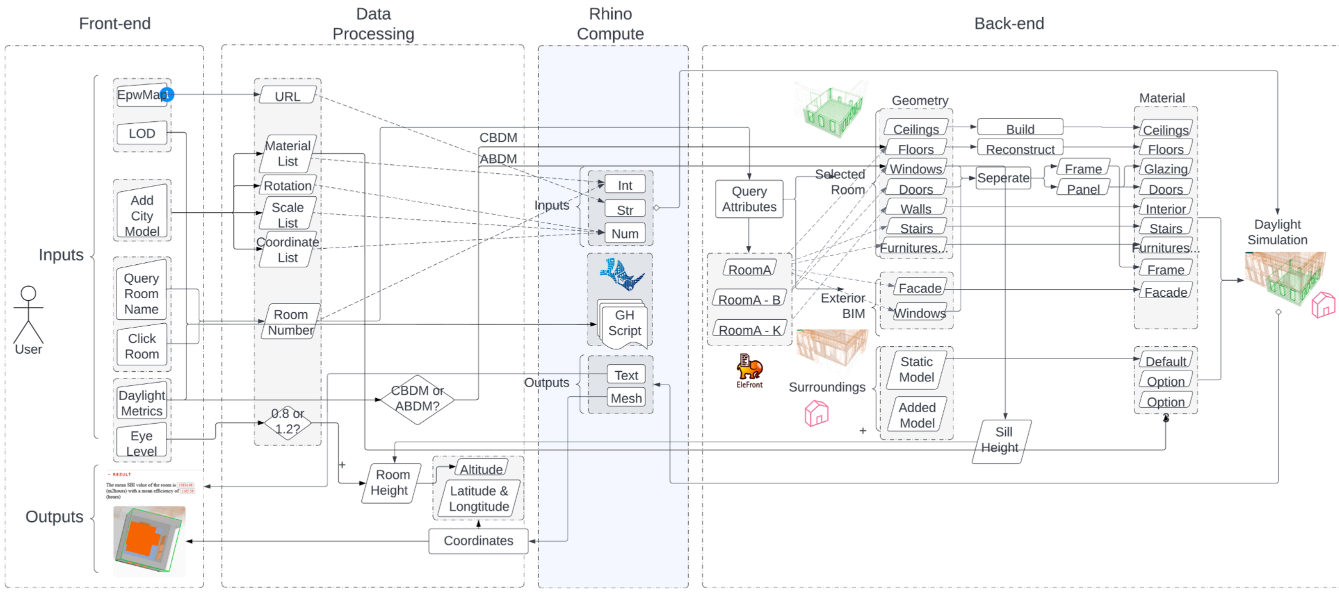

Fig. 3. Rhino Compute workflow for BIM element selection automation in daylight simulation.

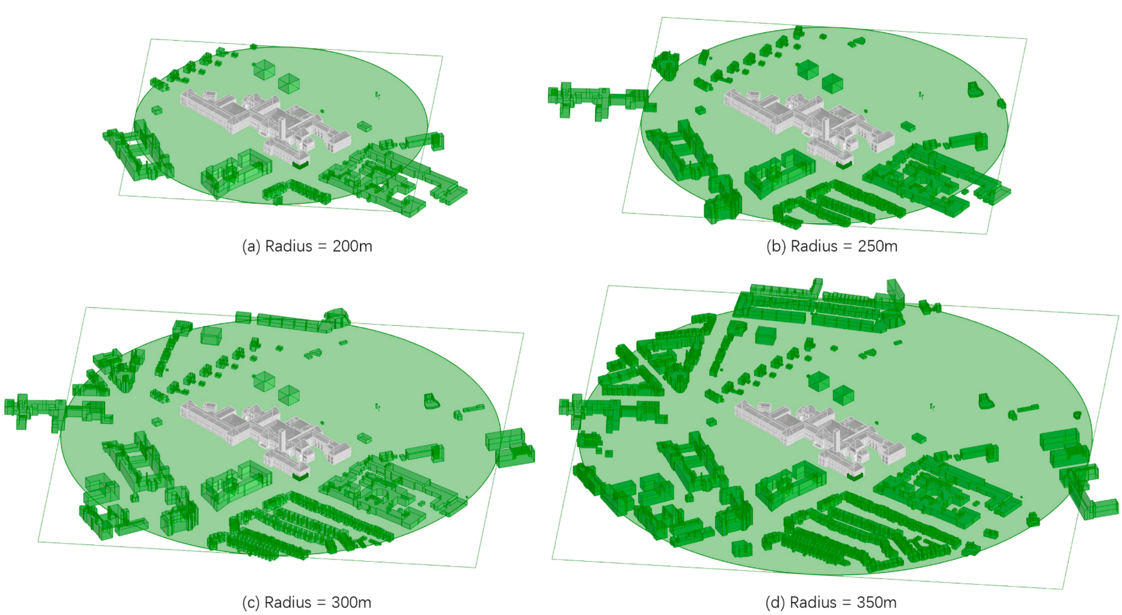

Fig. 4. Four radii for static 3D city model for case study.

as needed. The sixth and final step involves obtaining the simulation results, along with descriptions and comparisons with previous simulation results under the same conditions.

4.1.1. Simulation results comparison

In this interface, numerical results from each calculation are temporarily recorded for comparison with subsequent simulations. Initially, the result comparison column is blank. When the application is first run, this column remains empty. If it's the first calculation under a specific LOD or grid surface level option, it will display "This is the result of the first simulation in this case." If the LOD or grid surface level changes during the simulation, the results will be re-recorded (Fig. 6).

4.1.2. 3D city model incorporation

The 3D BAG model, as the 3D city model open data of the Netherlands, is imported in Mapbox using RhinoJSONCity. Upon initiating an HTTP request, data within the existing Mapbox scene is categorized by building typology and transmitted to the GH backend for geometric modifications: duplicating, rotating, scaling, and moving, to ensure synchronization with Mapbox data, and the final geometry is organized according to the materials to build the HB Shade component. Alterations to the Treebox source code are necessary to add attributes to each imported object, thereby enabling customization of their selectability, rotatability, draggability, and altitude adjustability, which is essential for implementing different levels of control between existing surrounding buildings and the added buildings. This application supports LOD options of 1.3 and 2.2, with the default setting at 2.2, which can be adjusted via a radio button interface.

4.1.3. Material selection

In the early stages of building planning, three alternative materials—float glass, reflective glass, and brick—were evaluated for façade

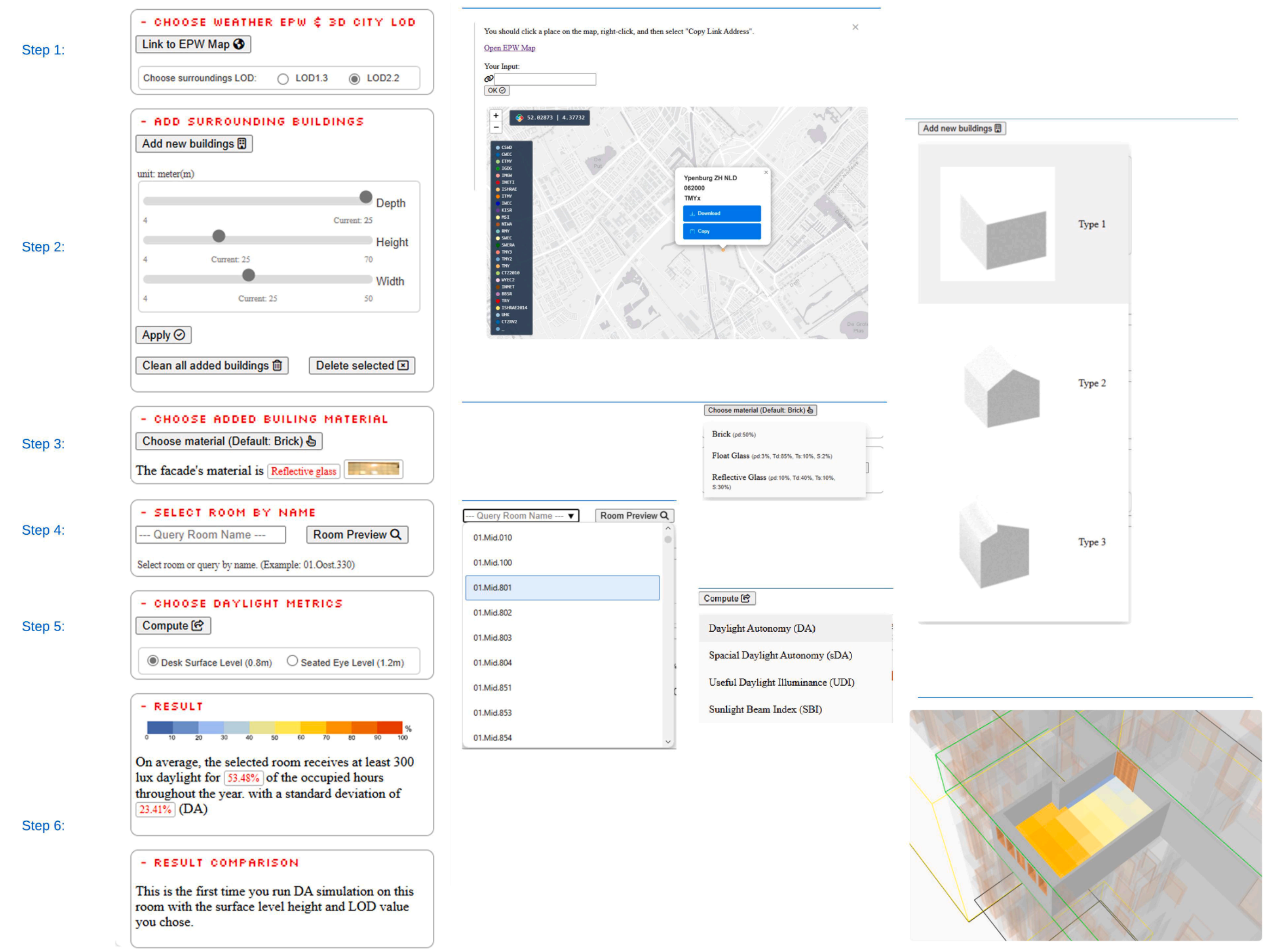

Fig. 5. User Interface.

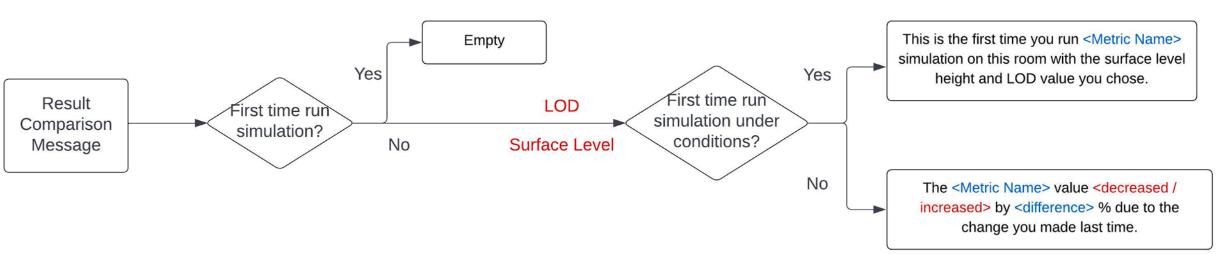

Fig. 6. Result comparison message showing in the application.

application in this case study. These materials provide a representative sample of local options, effectively showcasing the potential impact of new buildings. Notably, when using reflective glass, the HB Glass Modifier is not applied, as the material already includes predefined reflective properties. Instead, the HB Translucent Modifier[11] component is used, which allows for the customization of four key inputs: diffuse reflectance, transmitted diffuse, transmitted specular, and specular reflection, offering greater flexibility in material settings. The brick material is sourced from the library provided by the HB Search Modifiers. For materials with low transparency, such as brick, the critical parameter is diffuse reflectance. A typical reflectance value of 0.5 is used for this material. By default, brick is applied as the material for all newly added buildings. Additionally, the "HB Shade" is the lightest among HB objects, as it lacks boundary conditions or children and these material modifiers are also linked to the shade component.

4.1.4. Daylight metric selection

This application incorporates standard annual daylight metrics, including DA, sDA, UDI, and SBI, which proved (as shown in section 4.2) to have potential to supplant the conventional CBDM metrics at early design stages. Users select these metrics via a dropdown menu on the front-end, with the system recording a sequence number corresponding to the chosen metric and retrieving the appropriate file based on this identifier. The legend for each metric appears only after the user makes a

[11] Translucent modifier. https://docs.ladybug.tools/hb-radiance-primer/components/1_modifiers/translucent_modifier

selection from the dropdown menu. The coordinates of the mesh grid also differ depending on whether CBDM or ABDM is selected. CBDM is based on the indoor layout and requires floor coordinates, whereas ABDM is based on aperture and necessitates the coordinates of the windows. Given the regular type and distribution of windows in this case study, the window heights can be determined based on the floor heights. This application also provides comprehensive explanations for each metric to assist designers in comprehending the implications of the daylight metrics.

For simulating surface levels for CBDM metrics, two radio buttons are available, offering options of 0.8 m and 1.2 m, with the default set to 0.8 meters. A height of 1.2 m simulates daylight conditions at the average eye level of a seated person, accurately reflecting lighting for tasks like reading or computer work. Conversely, a height of 0.8 m assesses daylight performance on desk surfaces, helping designers evaluate natural light adequacy for tasks such as writing, reading, or using a computer. When the corresponding simulation grid is imported into Mapbox, the varying heights of the simulation surfaces will be reflected accordingly Fig. 7.

4.1.5. *Simulation results*

Fig. 8 provides an example of the simulation results for SBI metric, imported into Mapbox through Rhino Compute Appserver. It includes importing the simulation grid into the Mapbox interface (with the SBI based on the window positions) and displaying the numerical results in the result column of the sidebar.

4.2. *Analyses of simulation performance and daylight metric correlations*

A regular rectangular shape and an L-shaped layout were created for the correlation study. In addition, three aperture shapes were considered: rectangular, octagonal, and extended arch. The simulation also accounted for variations in window sill height, the number and position of apertures, and size of the rooms to achieve more generalized results. For each room configuration shown in Fig. 9, eight orientations were analyzed, both with shading (overhang extending 0.5 m horizontally from the facade) and without shading.

In the simulation, the surrounding geometries are modeled as a low-density urban area with low-rise buildings, reflecting the typical urban context of Delft.

The average simulation time for CBDM metrics was approximately 50 seconds per session for small rooms and 1.1 min per session for larger rooms. In contrast, the calculation time for ABDM metrics was negligible.

4.2.1. *DA and SBI-AM*

Based on the definition of ABDM metrics, shading was identified as a potential moderator of the results because it directly affects the aperture surface exposed to sunlight. To account for this influence, the dataset was divided into two groups: with shading and without shading, and separate correlation analyses were performed for each scenario. The following sections adopt this same structure.

Fig. 10 shows a moderate-strong positive association (R2 ≈ 0,619) between DA and SBI-AM under all modeled conditions. Higher DA consistently leads to higher SBI-AM values. The R2 values for with shading and without shading are 0,624 and 0,617 separately, both close to the combined value, suggesting that shading has little effect on the strength of the correlation.

While the R2 ≈ 0,619 values indicate a meaningful linear association, about 38% of the variance remains unexplained by DA alone. This residual scatter is consistent with the influence of other drivers, such as orientation, window-to-wall ratio, aperture shape and size, sill height, and room layout, which can all modulate SBI-AM outcomes independently of DA.

4.2.2. *sDA and SBI-AM*

Fig. 11 illustrates the correlation between sDA and SBI-AM, with $R^2 \approx 0.489$, indicating a moderate relationship, weaker than the DA vs. SBI-AM correlation analyzed earlier. This suggests that sDA explains only about 50% of the variance in SBI-AM, leaving roughly half influenced by other factors, making SMI-AM a less reliable predictor of sDA.

Given the definition of sDA, which includes threshold settings for annual occupied hours and indoor spatial distribution, in addition to target illuminance, a weaker correlation compared to DA is expected. The R^2 values for the shaded and unshaded scenarios (0.499 and 0.47) are close to the combined value, indicating again that shading has little effect on the strength of this relationship.

4.2.3. *UDI and SBI-AM*

Fig. 12 shows the correlation between UDI and SBI-AM. The overall

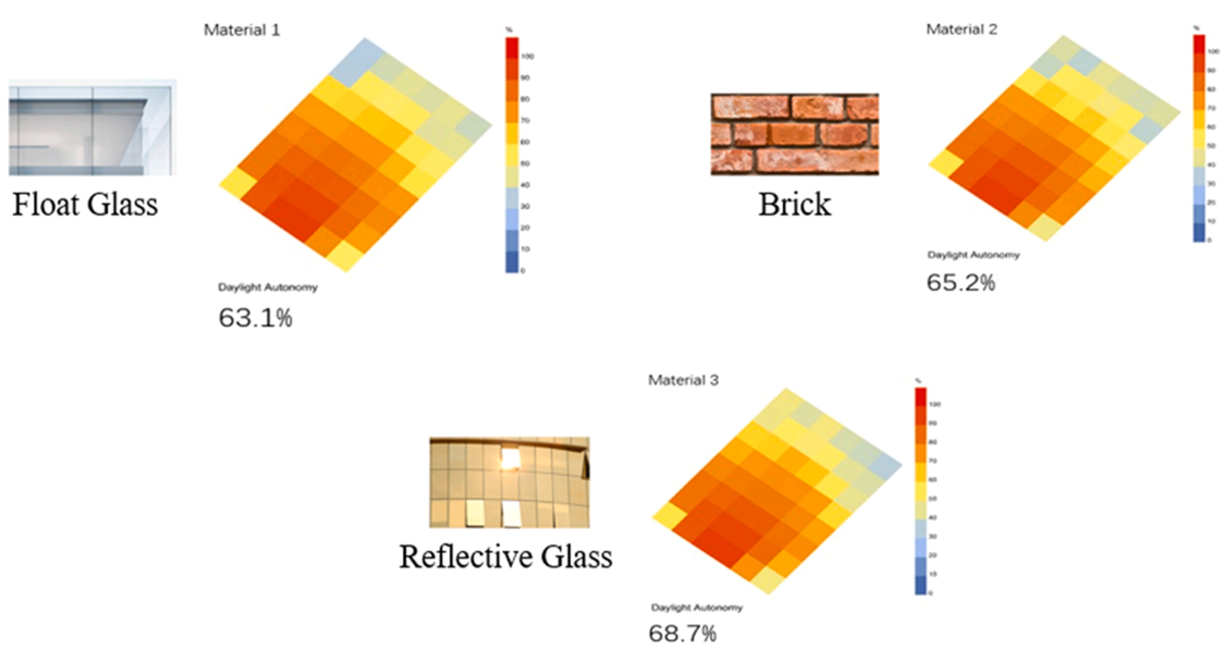

Fig. 7. Room DA value alterations due to material changes of obstruction.

Fig. 8. Simulation results for SBI metric.

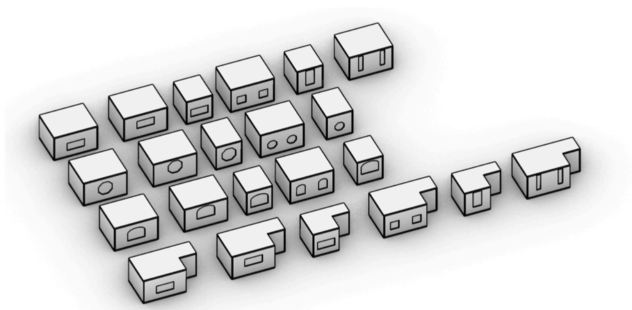

Fig. 9. Room layouts and aperture variations for correlation study.

R^2 value is 0,353, indicating a weak relationship between the two metrics. Shading significantly reduces the slope of the correlation, with the R^2 value decreasing from 0.404 to 0.303 under the shading condition. This indicates that shading is an important factor influencing the relationship and has a greater impact when UDI values are considered. SBI-AM is a poor predictor of UDI compared to DA or sDA because UDI measures illuminance within a useful range with both lower and upper thresholds, rather than total daylight exposure, which is more directly related to ABDM definition.

4.2.4. DA and Sky Lumen

Fig. 13 shows a weak linear relationship between DA and sky lumen. For a given sky lumen value, DA value spans a wide range, reflecting its strong dependence on orientation and solar path. In contrast, sky lumen remains relatively stable when the surrounding geometry density is unchanged across all directions. This variability makes it difficult to fit the data into a reliable regression model. Shading primarily shifts the level of sky lumen rather than strengthening the relationship, shading reduces the level but has little effect on correlation strength. Overall, sky lumen is a poor predictor of DA.

4.2.5. sDA and Sky Lumen

Similarly, as shown in Fig. 14, the correlation between sDA and sky lumen is also weak. The reason is comparable to the DA – Sky Lumen relationship, sky lumen is not orientation- or sun-path-based, and in a typical low-density urban context such as Delft, it tends to remain relatively constant for a given aperture in all directions. In contrast, sDA is highly dependent on orientation and includes an additional threshold for annual occupied hours. Shading has a significant impact on sky lumen because it directly obstructs a large portion of the view, but the correlation strength stays the same.

4.2.6. UDI and Sky Lumen

As shown in Fig. 15, UDI also shows a weak correlation with Sky Lumen. Shading significantly influences the relationship, and because all UDI values are above 25%, the data are less dispersed, resulting in a slightly higher R^2 value. This can be explained based on the definition, UDI considers only illuminance within a useful range, which makes it difficult to establish a strong correlation with sky lumen.

The correlation analysis between ABDM metrics and CBDM metrics reveals that among the ABDM metrics, DA shows the strongest association with SBI-AM. In contrast, sDA demonstrates a moderate correlation, while UDI exhibits only a weak relationship. These differences reflect their definitions: sDA incorporates indoor spatial distribution, and UDI focuses on a useful illuminance range rather than total daylight exposure. Across all cases, shading primarily affects the slope and intercept of the regression lines but has minimal influence on correlation

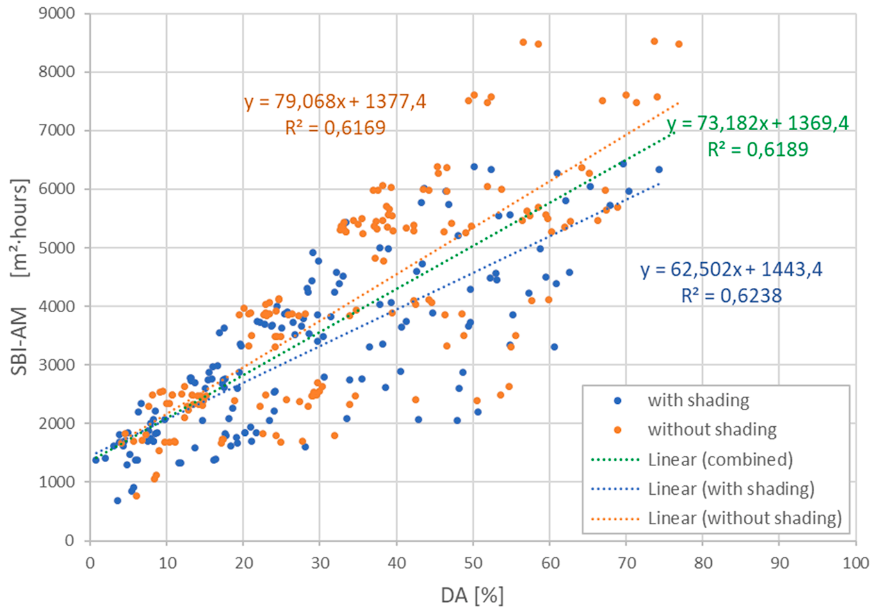

Fig. 10. Linear regression plot of relationship between DA and SBI-AM.

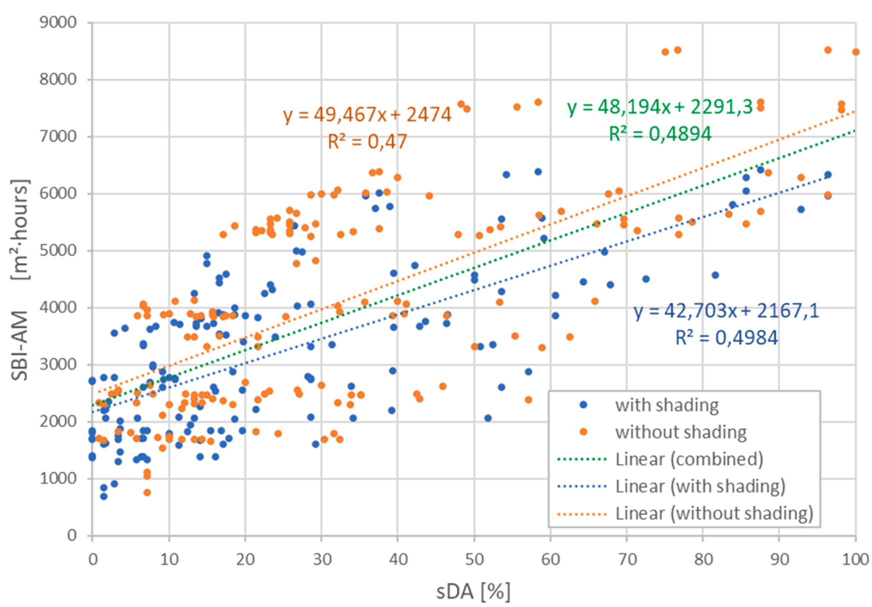

Fig. 11. Linear regression plot of the relationship between sDA and SBI-AM.

strength, except for UDI, where its impact is more pronounced. For Sky Lumen, correlations with DA, sDA, and UDI are consistently weak. This is expected because Sky Lumen depends on surrounding geometry and view obstruction rather than orientation or sun-path, whereas DA and sDA are highly orientation-dependent. Shading significantly reduces Sky Lumen values by blocking direct views but does not improve correlation strength.

Overall, SBI-AM has the potential to act as a proxy for DA results obtained at a later design stage, while the Sky Lumen cannot be directly linked to any CBDM metric. The role of Sky Lumen has more potential in relation to studies on view out. This hypothesis and the scalability of the SBI-DA correlation need further studies to be confirmed.

4.3. *Workflow performance analysis*

4.3.1. *3D city model LOD1 versus LOD2*

The DA metrics were analyzed to examine the impact of LOD variations on accuracy and computation time. For this analysis, 11 rooms, located on the outer part of the BK model, were selected to compare the DA metric results. The differences in simulation results are minimal across all rooms, indicating that LOD 1.3 closely approximates the results of LOD 2.2 (Fig. 16 and Fig. 17). However, the percentage differences in simulation time vary significantly, with certain rooms (e.g., Room 35, Room 227, and Room 378) showing substantial increases in time required for LOD 2.2 compared to LOD 1.3. In particular, rooms with large window openings or those facing detailed external geometry tend to be more sensitive to the increase in LOD, resulting in a more significant rise in simulation time due to the added complexity of light bounces and occlusion calculations in the ray tracing process (Fig. 18).

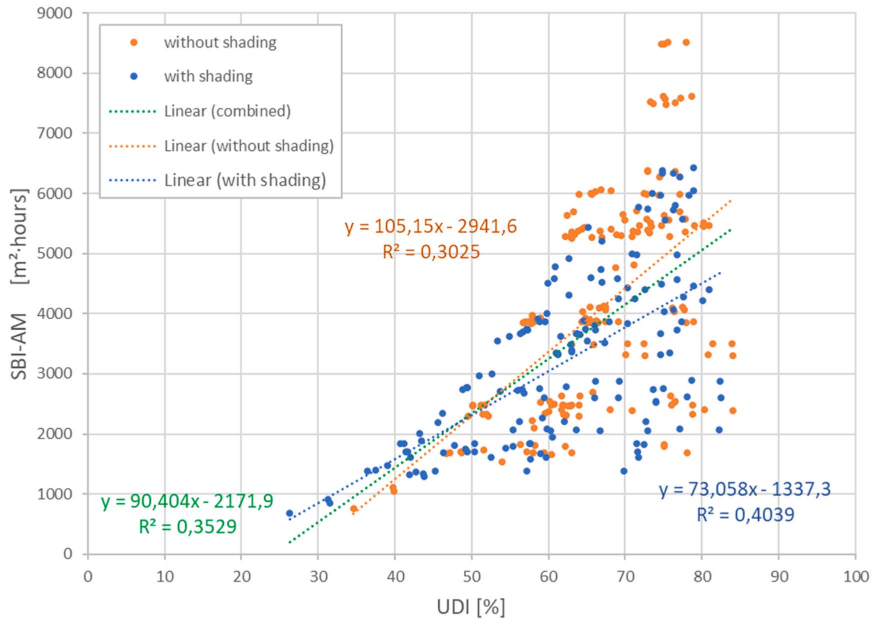

Fig. 12. Linear regression plot of the relationship between sDA and UDI.

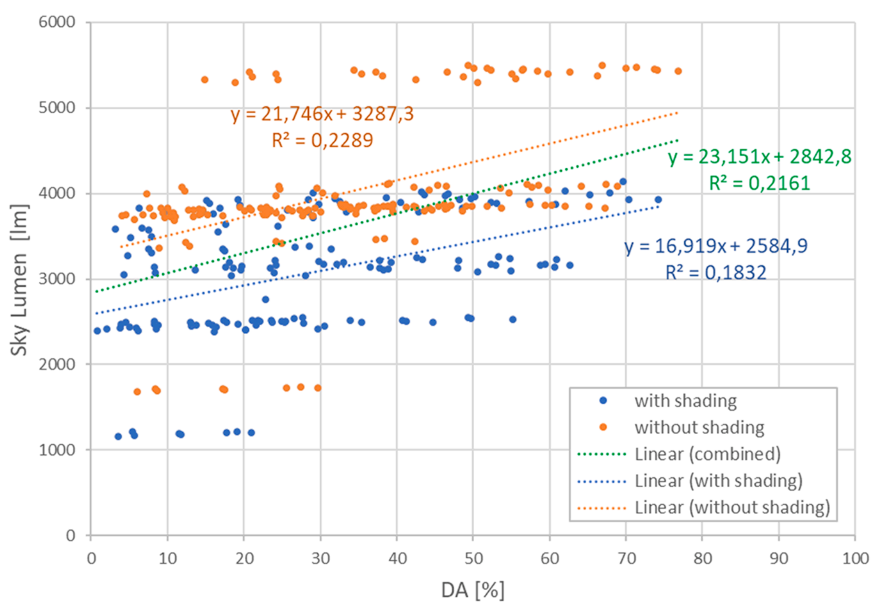

Fig. 13. Linear regression plot of relationship between DA and Sky Lumen.

This may be attributed to Delft's characteristics of low housing density and relatively short building heights. Despite the prevalence of pitched roofs in Delft, the impact of the building shapes is mitigated by the overall low density. Consequently, this finding might not be applicable to other locations, such as the city center of Amsterdam, where a higher density could result in a higher variation in simulation results between LOD 1.3 and LOD 2.2. In denser urban environments with taller buildings, tighter spacing, and more complex roof and façade geometries, higher LOD representations may exert a stronger influence on both daylight performance metrics and computational demand. While LOD 1.3 offers an efficient and sufficiently accurate option for the tested context, the proposed workflow allows users to adopt higher LODs when applying the method to high-density urban settings where geometric detail becomes more critical.

In conclusion, within this workflow, it is recommended to use LOD 1.3 for simulations as it delivers results comparable to LOD 2.2 without prolonging computational time. Nevertheless, users retain the flexibility to select either LOD 1.3 or LOD 2.2 for the final application.

4.3.2. Impact of 3D city model extent on daylight simulation performance

To estimate the impact of 3D city model extent on the daylight simulation performance, seven rooms of differing orientations were selected for the study. The mean DA value for each room was used as the evaluative metric for daylight simulation accuracy. All simulations were conducted with a LoD 1, a grid size of 0.6m, and a height of 0.8m, using the LOD 1.3 model from 3D BAG. Fig. 19 and Fig. 20 presents a comparative analysis of the mean DA values and computation times for different range radii.

Across all rooms, the DA mean values are quite consistent regardless of the range radius, indicating that increasing the radius beyond 200m doesn't significantly affect the accuracy of the daylight simulation results. This also suggests that smaller radii might be sufficient for

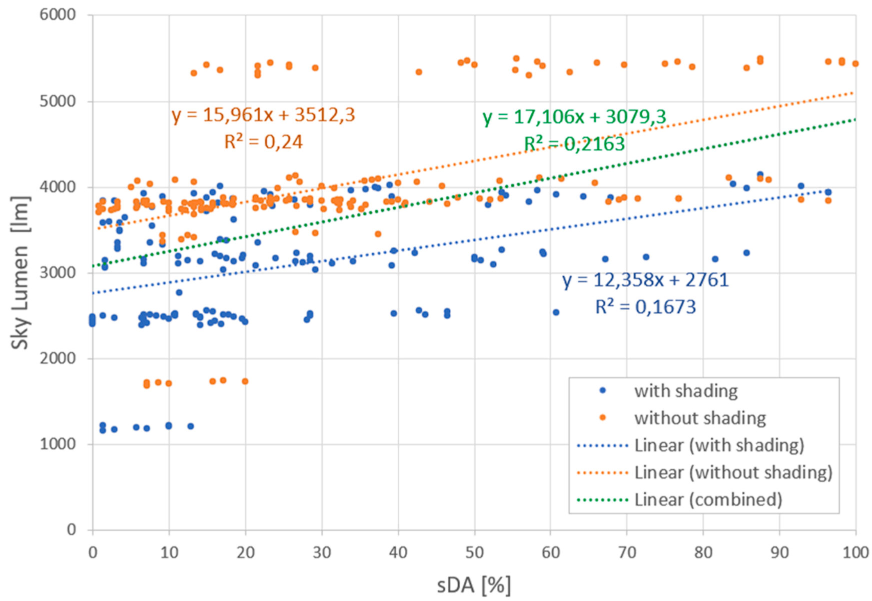

Fig. 14. Linear regression plot of relationship between sDA and Sky Lumen.

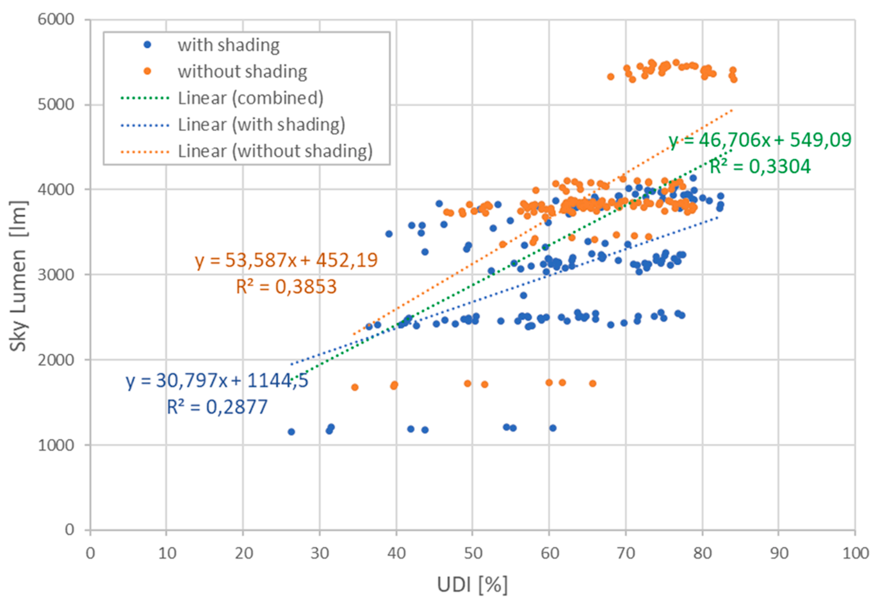

Fig. 15. Linear regression plot of relationship between UDI and Sky Lumen.

accurate daylight simulations, so in the GH script of all the metrics and LOD options, the 200m radius model is used for regular simulations due to its efficiency in computation time without compromising accuracy. As the range radius expands, computation time increases in most cases. Grasshopper records time with only one decimal place when it is more than 1 ', potentially obscuring minor variations. Despite this, the overall trend shows a clear upward trajectory, highlighting the increase in computational load as more model details are included.

The identified 200 m spatial extent should be interpreted as context-dependent and specific to the low- to mid-density urban morphology of Delft represented by the LOD 1.3 3D BAG model. In denser, high-rise urban environments, longer shadow-casting distances, reduced sky view factors, and complex inter-building interactions may extend the spatial influence on daylight performance beyond 200 m, potentially requiring larger model extents to fully capture relevant daylight interactions. While increasing the spatial radius leads to higher computational costs, the proposed workflow and web-based platform support flexible adjustment of the simulation extent, enabling users to balance accuracy and efficiency based on urban density, building height, and climatic context.

The impact of considering spatial context in daylight simulation has been investigated [39]. Our analysis of simulation radius effects reinforces literature on context dependency and computational burden in urban daylight modeling. Our observation that DA mean values remain stable beyond a 200 m radius suggests that expanding the spatial extent of urban context does not proportionally improve simulation accuracy but does increase computational load. This finding provides quantitative support for radius thresholds in daylight performance assessments, offering a practical guideline for optimizing computational resources without compromising analytical value.

The investigation into the effect of model LOD on Daylight Autonomy (DA) accuracy and computational effort confirms and extends recent observations that appropriate and context-specific geometric simplification can substantially improve performance simulation

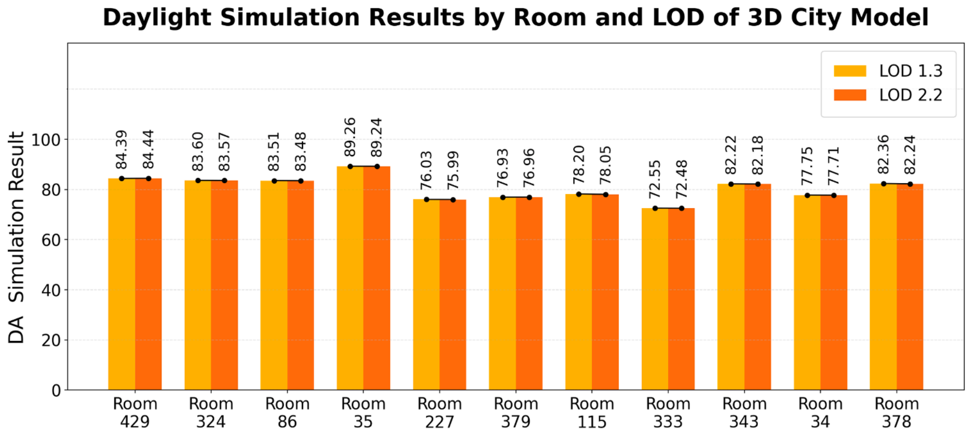

Fig. 16. Simulation accuracy comparison of LOD 2.2 and LOD 1.3 of static surrounding building models.

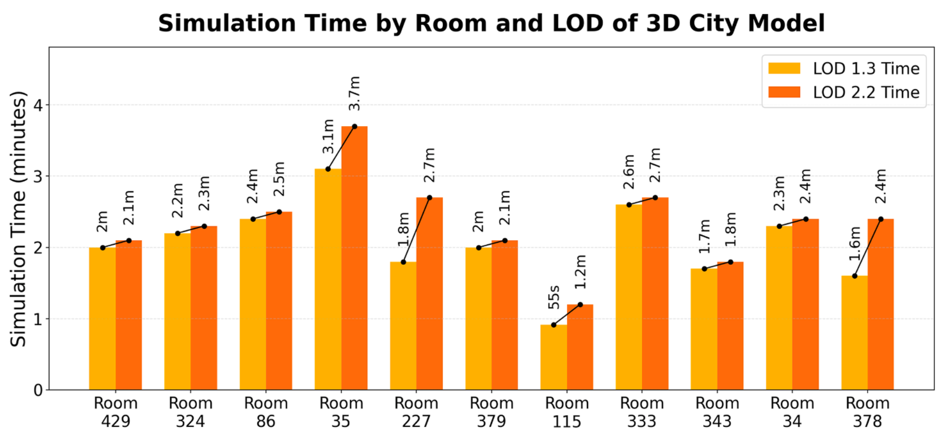

Fig. 17. Simulation time comparison of LOD 2.2 and LOD 1.3 of static surrounding building models.

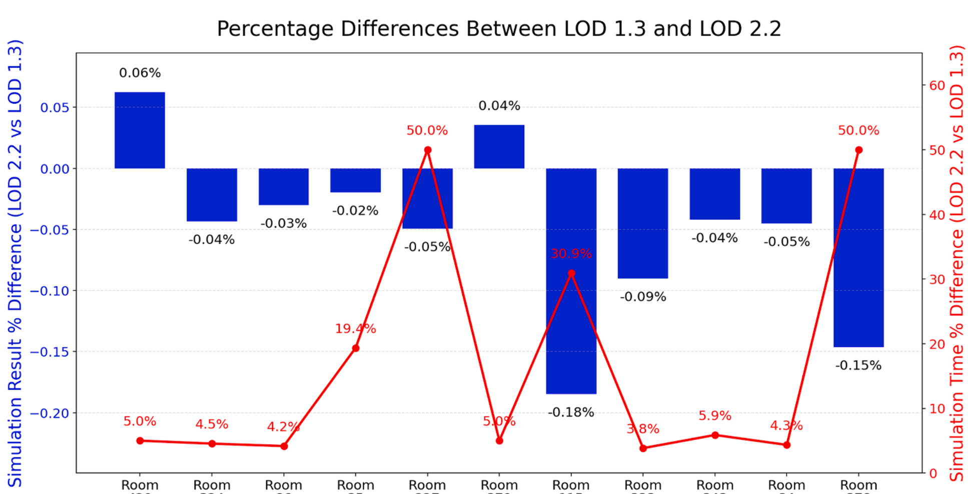

Fig. 18. Percentage variation in simulation time and accuracy between LOD 1.3 and LOD 2.2.

efficiency without significant loss of fidelity [52]. This aligns with emerging discussions on balancing model complexity and simulation practicality in urban daylighting studies. Whereas earlier research has often adopted higher-resolution models by default, without rigorous evaluation of their necessity in daylight metrics (e.g. [53,54]), our results provide empirical evidence that supports strategic LOD selection as a design parameter rather than an assumed prerequisite for accuracy. This outcome provides insight into the potential for streamlined integrated workflows for both planners and designers. This resonates with broader challenges in daylight simulation accuracy and validation, where geometrical representations and computational scalability are key themes in recent reviews [55]. The flexibility to choose either LOD 1.3 or 2.2 in the final application also offers practical adaptability across early-stage exploration and detailed refinement phases of urban design.

Furthermore, the successful deployment of MapboxGL as an interactive GIS platform for integrating BIM and urban models aligns with a

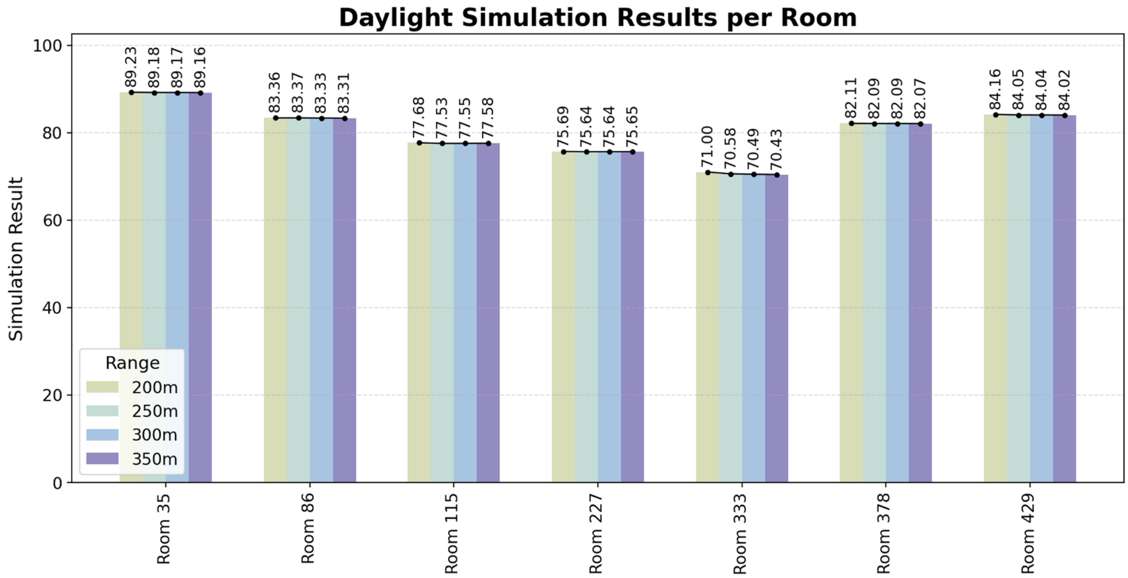

Fig. 19. Simulation accuracy comparison of different radius of spatial extent of surrounding buildings.

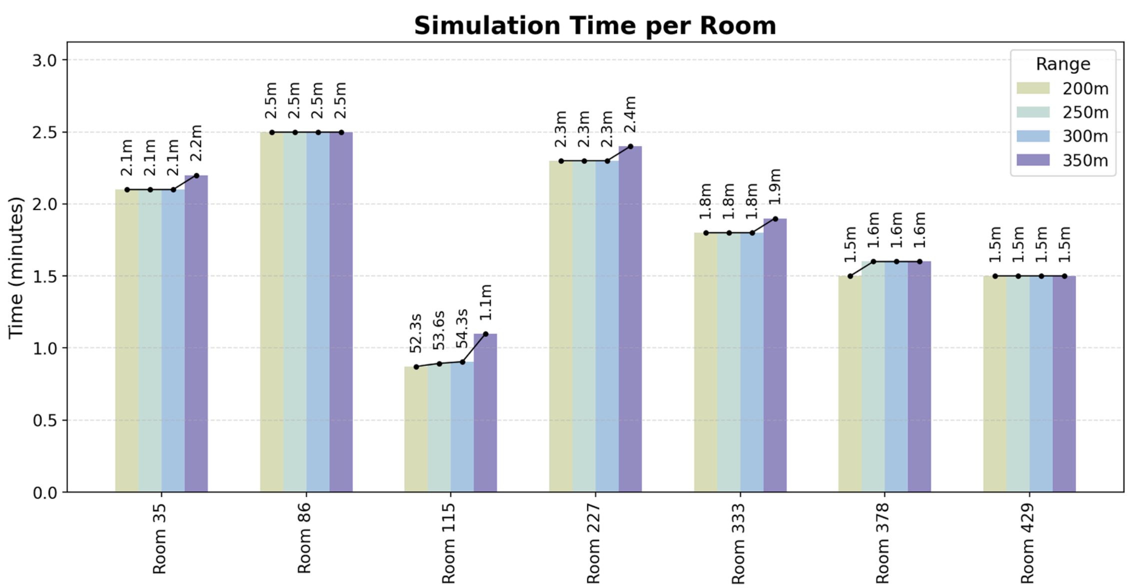

Fig. 20. Simulation time comparison of different radius of spatial extent of surrounding buildings.

growing trend towards web-based visualization environments that enhance user interaction and accessibility in environmental analysis workflow. For example, integration of BIM and GIS in a web viewer environment has been demonstrated for infrastructure asset management, enabling interactive exploration of combined model data [56,57] have employed Mapbox GL JS to render interactive maps in web-based systems for spatial visualization and analysis, demonstrating its viability for research-oriented geospatial applications (e.g., usage in a web-based interactive mapping system leveraging Mapbox GL JS for rendering and data handling.

The developed tool streamlines the daylight simulation workflow by providing an intuitive web-based interface. Users can add surrounding buildings through simple actions such as clicking, dragging, and dropping, without requiring prior knowledge of BIM, Rhino, or daylight simulation. The BIM model is pre-processed and loaded in a room-based format, while a Grasshopper script is automatically linked on the backend. Using cloud computing accelerates the simulation process compared to local execution on desktop Rhino and Grasshopper. This approach eliminates the need for Rhino installation and enables interactive access via a webpage, making it ideal for collaborative design reviews during early urban planning stages. For example, stakeholders can assess the impact of adding new buildings on daylight performance at the room level (or floor level with adjustments). The key advantage of this workflow is that a single expert can set up the system, allowing team members to run simulations and obtain results without specialized software or technical expertise.

5. Conclusions

In this study we have developed a web application for room-level daylight simulation considering its spatial context. This web application has been developed through an effective integration of BIM-GIS-daylight simulation triplet. This system integrates Grasshopper scripts, Rhino Compute, and MapboxGL to facilitate seamless interaction between BIM data, 3D city model, and simulation models, enabling flexible and customized daylight simulations. Furthermore, this system introduces the first interactive interface incorporating ABDM metrics that express façade daylight potential, in addition to the conventional CBDM metrics DA, sDA and UDI. In current BIM–GIS daylight workflows, performance is typically assessed using CBDM metrics derived from ray-tracing simulations. Although accurate, these methods are computationally intensive and therefore difficult to implement in large-scale or iterative processes. To date, ABDM has not been incorporated into BIM–GIS workflows.

This study investigated whether ABDM-based metrics could provide meaningful information within a BIM–GIS daylight assessment framework and function as alternative or supporting indicators in practice. The results indicate that their applicability is metric-dependent: SBI-AM demonstrated a strong correlation with DA, suggesting its potential as an early-stage proxy in contexts where ray-tracing simulations are impractical or overly time-consuming. Accordingly, the final application integrates SBI as a selectable daylight simulation metric that can reliably provide a proxy of indoor daylight performance at early design stages. While ABDM cannot replace CBDM, specific metrics such as SBI-AM may complement simulation-based approaches in computationally constrained workflows, or serve as additional daylight indicators during early design phases when detailed indoor information is not yet available.

Sky Lumen was found to be weakly correlated with the investigated CBDM metrics, as less dependent on orientation and sun position. At the moment, it was therefore not implemented in the final application. It might be however a metric of interest for studies on view and should be investigated further in future research.

MapboxGL demonstrated to be an effective GIS platform for integrating BIM models in room-level daylighting simulations, offering a user-friendly interactive system for efficient manipulation of newly added buildings. The 3D city model of the Netherlands, as open data, is served in the platform at two different detail levels, to include the spatial context and facilitate their leverage on daylight simulation based on the required detail level and computational time for different applications. The integration of Rhino Compute technology facilitates user interaction, transfer, and access to both geometric and numerical daylighting data seamlessly.

The application offers practical value to multiple stakeholders. Urban planners and architects can leverage the application to assess and optimize daylight performance in building designs, enhancing energy efficiency and occupant comfort. City authorities and policymakers can use it for informed sustainable urban planning strategies, ensuring that new developments maximize natural light while minimizing energy consumption. Environmental researchers, sustainability consultants, developers, and construction professionals benefit from actionable insights into daylight availability across urban environments, promoting smarter and more sustainable urban design.

Software availability

Name of software: Cloud-based room-centric daylight simulation tool for environment design

Developer: Yangyu Liu, TU Delft, liuyangyu82@outlook.com

Date first made available: July 2024.

Software required: Web browser, Visual Studio, Rhino, Node JS

Program Language: JavaScript, Python, C#, HTML/CSS

Source Code: Accessible to anyone at https://github.com/ottertje/compute.rhino3d.appserver.

Cost: Free.

CRediT authorship contribution statement

Yangyu Liu: Writing – original draft, Visualization, Validation, Software, Methodology, Investigation, Formal analysis, Data curation, Conceptualization. **Eleonora Brembilla:** Writing – review & editing, Supervision, Methodology, Conceptualization. **Azarakhsh Rafiee:** Writing – review & editing, Supervision, Methodology, Conceptualization.

Declaration of competing interest

The authors declare that they have no known competing financial interests or personal relationships that could have appeared to influence the work reported in this paper.

Supplementary materials

Supplementary material associated with this article can be found, in the online version, at doi:10.1016/j.buildenv.2026.114376.

Data availability

Data will be made available on request.

References

[1] Wedia. (n.d.). *Amsterdam unveils plans to build 20.000 new homes in existing neighbourhoods*. IamExpat. https://www.iamexpat.nl/housing/real-estate-news/amsterdam-unveils-plans-build-20000-new-homes-existing-neighbourhoods.
[2] P. Chynoweth, Progressing the rights to light debate, Struct. Surv. 23 (4) (2005) 251–264, https://doi.org/10.1108/02630800510630439.
[3] V.S. Rajus, N.A. Risopatron, W. O'Brien, G. Wainer, S. Fai, Mitigating the negative impact of new buildings on existing buildings' user comfort—A case study analysis, Simulation. 99 (11) (2022) 1095–1115.
[4] V.R.L. Verso, G. Antonutto, S. Torres, Sunlight-daylight signature: a novel concept to assess sunlight and daylight availability at urban scale, J. Daylighting 10 (2) (2023) 136–152.
[5] Y. Wang, J. Guo, Y. Jiang, C. Sun, Multi-objective optimization of buildings in urban scale for early stage planning and parametric design, Sustain. Cities. Soc. 113 (2024) 105714.
[6] F. Vecchi, U. Berardi, Solar analysis for an urban context from GIS to block-scale evaluations, Energy Policy 184 (2024) 113884.
[7] E. Brembilla, J. Mardaljevic, Climate-based daylight modelling for compliance verification: benchmarking multiple state-of-the-art methods, Build. Environ. 158 (2019) 151–164.
[8] J. Mardaljevic, Aperture-based daylight modelling: introducing the 'View Lumen, in: 16th IBPSA International Conference and Exhibition: Building Simulation 2019, 2019. Rome (Italy)Sep 2 –4, 2019.
[9] M. Taghizadeh, N. Gentile, P. Mattsson, M.C. Dubois, Energy impact of integrative lighting: A systematic literature review, Energy Build. (2025) 115920.
[10] N.R. Oghazi, T. Jusselme, M. Andersen, Daylight and carbon interactions: an explorative method to reconcile daylight performance and carbon budget constraints, Build. Environ. 262 (2024) 111777.
[11] M. Knoop, O. Stefani, B. Bueno, B. Matusiak, R. Hobday, A. Wirz-Justice, K. Martiny, T. Kantermann, M. Aarts, N. Zemmouri, S. Appelt, B. Norton, Daylight: what makes the difference? Light. Res. Technol. 52 (3) (2019) 423–442.
[12] M. Fernandez-Antolin, J. Del-Río, F. Del Ama Gonzalo, R. Gonzalez-Lezcano, The relationship between the use of building performance simulation tools by recent graduate architects and the deficiencies in architectural education, Energies 13 (5) (2020) 1134.
[13] M. Fernandez-Antolin, J.M. Del Río, R.A. González-Lezcano, Building performance simulations and architects against climate change and energy resource scarcity, Earth 3 (1) (2022) 31–44.
[14] A. Schlueter, F. Thesseling, Building information model based energy/exergy performance assessment in early design stages, Autom. Constr. 18 (2) (2009) 153–163.
[15] Shoshev, M. (2022). From building information models to Building Performance Simulation: parametric workflow for high performance building envelope design for daylight and glare analysis (Doctoral dissertation, Politecnico di Torino).
[16] G. Ward Larson, R.A. Shakespeare, Rendering with Radiance: The art and science of lighting visualization, Morgan Kaufmann Publishers, 1998.
[17] M. Alenius, M. Lundgren, Architectural repertoire and daylight metrics, NA 32 (1) (2020).
[18] BRE, Site layout planning for daylight and sunlight: A guide to good practice, 2nd ed., Building Research Establishment, 2011.
[19] N. Nasrollahi, E. Shokri, Daylight illuminance in urban environments for visual comfort and energy performance, Renew. Sustain. Energy Rev. 66 (2016) 861–874.
[20] J. Mardaljevic, Examples of climate-based daylight modelling, in: CIBSE national conference, 2006, pp. 1–11.
[21] E. Ukpong, F.O. Uzuegbunam, E.O. Ibem, E. Udomiaye, Daylighting performance evaluation in tropical lecture rooms: a comparative analysis of static and climate-based metrics, J. Build. Eng. 103 (2025) 112044.
[22] A. Bagheri, H. Sanaieian, M. Ali Khanmohammadi, H. Yazdani, Investigating the influence of Atrium wall inclination on daylight performance in different latitudes using climate-based daylight modeling, J. Arch. Eng. 31 (1) (2025) 04025003.

[23] M. Sudan, R.G. Mistrick, G.N. Tiwari, Climate-based daylight modeling (CBDM) for an atrium: an experimentally validated novel daylight performance, Sol. Energy 158 (2017) 559–571.
[24] J. Mardaljevic, E. Brembilla, Aperture-based daylight modelling: evaluating the airmass refinement for the sunlight beam index, in: Building Simulation Conference Proceedings, 2021.
[25] USGBC, LEED Reference Guide for Building Design and Construction, U.S. Green Building Council, 2013.
[26] IES, IES LM-83-12: approved method: IES spatial daylight autonomy (sDA) and annual sunlight exposure (ASE), Illum. Eng. Soc. (2012).
[27] A. Nabil, J. Mardaljevic, Useful daylight illuminance: a new paradigm for assessing daylight in buildings, Light. Res. Technol. 37 (1) (2005) 41–57.
[28] J. Mardaljevic, N. Roy, The sunlight beam index, Light. Res. Technol. 48 (1) (2016) 55–69.
[29] J. Mardaljevic, The implementation of natural lighting for human health from a planning perspective, Light. Res. Technol. 53 (5) (2021) 489–513 [29] Alisherbek, N. (2021). Development of Urban Development in the Territory of Uzbekistan. Central Asian Journal of Theoretical & Applied Sciences, 2(10), 24-26.
[30] Mcneel. (n.d.). *GitHub - mcneel/compute.Rhino3d.Appserver: A node.Js server for solving grasshopper definitions on Rhino Compute*. GitHub. https://github.com/mcneel/compute.rhino3d.appserver.
[31] K. Pantazatou, J. Kanters, P. Olsson, J.L. Nyborg, L. Harrie, Input data requirements for daylight simulations in urban densifications, Urban. Inform. 2 (1) (2023).
[32] R. Peters, B. Dukai, S. Vitalis, J. Van Liempt, J. Stoter, Automated 3D reconstruction of LOD2 and LOD1 models for all 10 million buildings of the Netherlands, Photogramm. Eng. Remote Sens. 88 (3) (2022) 165–170, https://doi.org/10.14358/pers.21-00032r2.
[33] D.A. Leon, B. Pachuca. https://medium.com/@kpfui/bridging-data-science-and-architectural-practice-aceb3f23fd95, 2022.
[34] D. Ronald, Killer product — A Rhino3D product analysis - spatiomatics -medium, Medium (2021). https://medium.com/spatiomatics/killer-product-a-rhino3d-productanalysis-2f90ebfd9465.
[35] S. Pelden, S. Banihashemi, S.R. Mohandes, M. Arashpour, M. Kalantari, Enhancing infrastructure planning and design through BIM-GIS integration, Struct. Infrastruct. Eng. (2025) 1–20.
[36] Y. Song, X. Wang, Y. Tan, P. Wu, M. Sutrisna, J.C. Cheng, K. Hampson, Trends and opportunities of BIM-GIS integration in the architecture, engineering and construction industry: A review from a spatio-temporal statistical perspective, ISPRS. Int. J. Geoinf. 6 (12) (2017) 397.
[37] A. Rafiee, E. Dias, S. Fruijtier, H. Scholten, From BIM to geo-analysis: view coverage and shadow analysis by BIM/GIS integration, Procedia Environ. Sci. 22 (2014) 397–402.
[38] S. Amirebrahimi, A. Rajabifard, P. Mendis, T. Ngo, A BIM-GIS integration method in support of the assessment and 3D visualisation of flood damage to a building, J. Spat. Sci. 61 (2) (2016) 317–350.
[39] D. Koster, A. Rafiee, E. Brembilla, The effect of urban density on compliance with indoor visual and non-visual daylight targets: a Dutch case study, Sustain. Cities. Soc. (2025) 106149, https://doi.org/10.1016/j.scs.2025.106149.
[40] N. Forouzandeh, E. Brembilla, L. Nan, J. Stoter, A. Jakubiec, Influence of geometrical levels of detail and inaccurate material optical properties on daylight simulation, Energy Build. 306 (2024) 113924.
[41] A. de Waal, M. Weaver, T. Day, B. van der Heijden, Silo-busting: overcoming the greatest threat to organizational performance, Sustainability. 11 (23) (2019) 6860, https://doi.org/10.3390/su11236860.
[42] Computational Modelling Group, BIM-GIS integration: Knowledge graphs in a world of data silos (Preprint No. 311), University of Cambridge, 2023. Retrieved from, https://como.ceb.cam.ac.uk/media/preprints/c4e-preprint-311.pdf.
[43] G. Celeste, M. Lazoi, M. Mangia, G. Mangialardi, Innovating the construction life cycle through BIM/GIS integration: a review, Sustainability. 14 (2) (2022) 766.
[44] H.Y. Quek, F. Sielker, J. Akroyd, A.N. Bhave, A. Von Richthofen, P. Herthogs, C. Van Der Laag Yamu, L. Wan, T. Nochta, G. Burgess, M.Q. Lim, S. Mosbach, M. Kraft, The conundrum in smart city governance: interoperability and compatibility in an ever-growing ecosystem of digital twins, Data Policy. 5 (2023).
[45] D. Shkundalov, T. Vilutienė, Building management system in WebBIM environment, in: 11th International Conference "Environmental Engineering, 2020. Vilnius Gediminas Technical University, Lithuania, 21–22 May 2020.
[46] Wallabyway, GitHub - wallabyway/mapboxRevit: view revit models inside Mapbox, GitHub (2019). https://github.com/wallabyway/mapboxRevit?tab=readme-ov-file.
[47] Helenkwok, GitHub - helenkwok/bim-gis-viewer: a submission to IFC.Js hackathon, GitHub, https://github.com/helenkwok/bim-gis-viewer, 2023.
[48] Kasten, F. (1965). A new table and approximation formula for the relative optial air mass. 14(2), 206–223.
[49] A.B. Meinel, M.P. Meinel, Applied Solar Energy: An introduction, Addison-Wesley Publishing Company, 1976.
[50] M. Inanici, Applications of image based rendering in lighting simulation: development and evaluation of image based sky models. https://www.semanticscholar.org/paper/APPLICATIONS-OF-IMAGE-BASED-RENDERING-IN-LIGHTING-Inanici/48f1f521a95aaf70658db1e9b6e224409c9d0baf, 2009.
[51] Y. Zheng, A. Merchant, J. Laninga, Z.X. Xiang, K. Alshaebi, N. Arellano, D.H. Sun, Comparison of characteristics of BIM visualization and interactive application based on WebGL and game engine. The International archives of the photogrammetry, Remote Sens. Spat. Inf. Sci. 48 (2023) 1671–1677.
[52] J. Potočnik, L. Pajek, M. Košir, Experimental investigation of the impact of model complexity on indoor daylight spectral simulations, Dev. Built Environ. 20 (2024) 100543.
[53] R. Wróżyński, K. Pyszny, M. Wróżyńska, Reaching beyond GIS for comprehensive 3D visibility analysis, Landsc. Urban. Plan. 247 (2024) 105074.
[54] L. Harrie, J. Kanters, K. Mattisson, P. Nezval, P.O. Olsson, K. Pantazatou, H. Fan, 3D city models for supporting simulations in city densifications. The international archives of the photogrammetry, Remote Sens. Spat. Inf. Sci. 46 (2021) 73–77.
[55] M. Nazari, B. Matusiak, Daylighting simulation and visualisation: navigating challenges in accuracy and validation, Energy Build. 312 (2024) 114188.
[56] V.V. Hung, N.C. Phuong, Integration of BIM and GIS on web viewer environment for Tan Cang station asset management, Transp. Res. Procedia 85 (2025) 281–288.
[57] M.O. Mete, T. Yomralioglu, Implementation of serverless cloud GIS platform for land valuation, Int. J. Digit. Earth. 14 (7) (2021) 836–850.